Failure characteristics of cladding tubes under RIA conditions through electromagnetic forming

Maurice Leroy[1)], Aurore Parrot[2)], and Sylvain Leclercq[2)]

1) Laboratoire FORSEM, IUT de Nantes, 3 rue du maréchal Joffre, 44041 Nantes cedex 1, France
2) EDF R&D, Material and Mechanics of Components dept., 77818 Moret-Sur-Loing, France

ABSTRACT

In the frame of actions for improving the safety of its nuclear power plants, Électricité de France needs to build the mechanical criteria ensuring the clad integrity for several operating conditions. As concerns the rod ejection accidents, an analytical mechanical criterion has recently been developed in order to assess the risk of failure during an RIA event. The derivation of this analytical criterion requires the use of an experimental data base, which is not always perfectly representative of the RIA full-scale test loading conditions. The aim of this study is to develop an experimental set up in order to characterize the fracture behavior of cladding tubes under RIA conditions (equibiaxial tension and high strain rates). The developed experimental set up is based on electromagnetic forming. The development of the test is delicate but leads to repeatable results with a controlled strain biaxiality ratio and very high strain rates. The experimental results are in good agreement with the first simulations of the test.

INTRODUCTION

In the frame of actions for improving the safety of its nuclear power plants, Electricité de France needs to build the mechanical criteria ensuring the clad integrity for several operating conditions. As concerns the rod ejection accidents, the French code SCANAIR [1] is used by EDF to perform the surveillance of RIA (Reactivity Initiated Accident) studies. The code provides some thermal, mechanical, irradiation, chemical data that are used to evaluate the risk of rod failure during an RIA at high burnup. The risk of failure is assessed by comparing the rod data provided by SCANAIR with the "safety domain" previously proposed by EDF [2]. This domain is made on the basis of the results of the CABRI REP-Na tests [3]. Therefore the main drawback of the "safety domain" is that it is impossible to extrapolate the results beyond its limits. Thus EDF has decided to develop a new methodology, based on an analytical mechanical criterion (the Critical Strain Energy Density – CSED) which has already been used by EPRI [4]. The derivation of this analytical criteria requires the use of an experimental data base, which is not always perfectly representative of the RIA full-scale test loading conditions. Experimental data provided by several programmes (PROMETRA [5], EPRI [4]) have been interpreted in order to become consistent with experimental tests like REP-Na ones, and a scheme for the derivation of CSED representative of RIA themomechanical conditions has been proposed [6, 7].

In order to consolidate the built criteria, the aim of our study is to develop an experimental set up in order to characterize the fracture behavior of cladding tubes under RIA conditions. During an RIA, the cladding is in equibiaxial tension ($\varepsilon_{zz}/\varepsilon_{\theta\theta} = 1$) due to the loading imposed by the thermal expansion of the pellet. The typical strain rate expected for the cladding is $5s^{-1}$. The developed experimental set up will be based on electromagnetic forming.

EXPERIMENTAL PROCEDURE AND RESULTS

Electromagnetic forming (EMF) is a dynamic, high strain rate forming method. In this process, deformation of the workpiece is driven by the interaction of a current generated in the workpiece with a magnetic field generated by a coil adjacent to the workpiece. The interaction of these two fields results in a material body force which acts on all parts of the specimen equally.

In the developed experimental set up, a capacitor, charged to a certain voltage, is discharged through a solenoid around which a high conductivity driver surrounded by the tested specimen has been placed. The counter-rotating current induced in the driver interacts with the magnetic field created by the solenoid, producing a large outward radial force and causing it to expand the cladding tube. In order to control the strain biaxiality ratio during the test, the driver and the surrounding specimen are inserted into a die including an hollowing where the deformation will take place. The hollowing shape will control the strain biaxiality ratio. A scheme of the experimental set up is presented on Figure 1 (due to symmetry consideration, only one quarter of the experimental set up has been drawn).

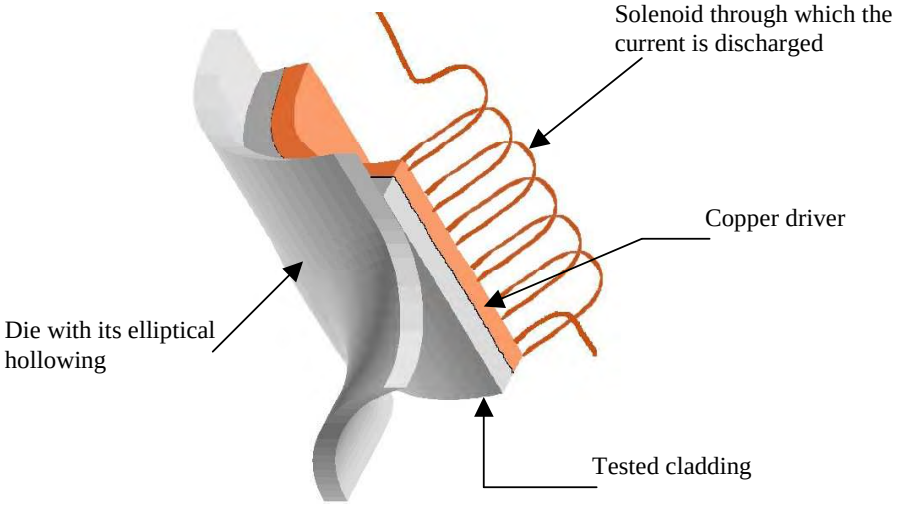

Figure 1. Scheme of the experimental set up.

The energy inserted into the system is controlled by the capacitor voltage discharged into the solenoid. The used voltage varies between 0 and 9kV. The solenoid is made of a copper wire with a 1mm diameter, winded into 10 to 15 spirals. During the current discharge, the solenoid is submitted to inter-spirals forces which tend to squeeze it. In order to apply the desired loading to the specimen, the solenoid must withstand this forces long enough. To prevent the early solenoid destruction, it is coated into a ceramic.

The dies are made of a beryllium copper alloy. Several dies with different hollowings have been used in order to make the strain biaxiality ratio vary. The dies characteristics are given in Table 1. In order to prevent cutting of the specimen to the shape of the hollowing, the intersection between the hollowing and the die has an adjusted curvature radius chosen according to preliminary testing.

A grid (500x500µm²) was engraved on most of the specimens in order to measure fracture strains after testing. The amperages in the solenoid can reach hundreds of kilo-amperes. These amperages are measured thanks to a Rogorwsky coil connected up an integrating circuit delivering the signal to an oscilloscope. Finally, the hoop strain rate at the centre of the hollowing can be measured either with a laser extensometer process or with a high speed digital camera.

For the first test series, the tested material is a CWSR Zircaloy-4 alloy at the reception state. The specimen are taken from a fuel rod, the outer diameter is 9.5mm, the thickness is 570µm and the specimen are 25 or 50mm high. The hoop strain rates are not yet measured and the measure of the amperage in the solenoid was performed on a single test. Table 1 presents the experimental results obtained during this first series.

The tests results are reproducible in spite of the experimental difficulty. Some of the tests must have been rejected because of a bad positioning of the coil leading to a decentred strain dome. The majority of the cracking observed started off the engraving little deep though it is (see Figure 2b). Nevertheless it is likely that the crack initiation is not very altered by the engraving. In order to verify this hypothesis, for the next test series, pebble dash painting will be applied on a few specimen in order to determine fracture strains through picture correlation.

Figure 2 shows macrographic observations of specimen after testing. Figure 2a shows the strain dome obtained with the 5x4 and 4x5 dies without any reworking of the curvature radius. Cutting of the specimen at the hollowing edges can be observed. Figure 2b shows specimen tested with the 5x4 die after reworking. No more cutting at the hollowing edges is observed and axial as well as hoop cracking are noticed on the strain dome.

The 4x5 is the most interesting die for the desired application. Indeed it leads to the strain biaxiality ratios at crack initiation ($\varepsilon_{zz}/\varepsilon_{\theta\theta} \approx 0.5$) the closest from those expected during an IRA event. Moreover axial and hoop cracking are observed on the strain dome and during a RIA test, at high burnup, the rod failure mode is an axial splitting of the cladding under a predominant hoop loading. Finally, the estimated strain rate during the test is $10^3 s^{-1}$ which is in an interesting range.

The 5x4 die leads to lower strain biaxiality ratios and hoop cracking. The biaxiality ratio has not been measured on the 5x3 die and only hoop cracking was observed. The 7x7 die gives strain biaxiality ratio in the region of those obtained on classical ring tests. These dies are interesting for the study of the influence of the strain biaxiality ratio on the fracture properties.

The next test will mainly be performed with the 4x5 and 5x4 die. Other zircaloy alloys at the reception state and in hydrided conditions will be tested in order to look at hydrides influence on fracture strains. Fracture strains will also be evaluated through picture correlation and the strain rate measurement will be set up. The experimental design has been designed in order to make test in temperature, tests at 350°C are foreseen.

Table 1. Experimental results

Die*	Curvature radius**	Generator supplying voltage	Axial strain in the centre of the hollowing	Hoop strain in the centre of the hollowing	Biaxiality ratio in the centre of the hollowing	Experimental observation
4mm x 5mm	2mm	6,2kV	0.1	0.13	0.77	Cutting to the hollowing edges and initiation of hoop cracking
	$2mm^{+}$	6,5kV	0.012 0.034	0.15 0.16	0.08 0.2125	No cracking initiation
5mm x 4mm	2mm	6,2kV	0.045	0.18	0.25	Cutting to the hollowing edges and initiation of hoop cracking
	$2mm^{+}$	6,5kV	0.065	0.135	0.48	Hoop cracking
	$2mm^{++}$	6,7kV	0.07	0.142	0.49	Small cutting to the hollowing edges
	$2mm^{+++}$	6,7kV	0.06	0.155	0.39	Axial and hoop cracking
	$2mm^{+++}$	6,7kV	0.08	0.17	0.47	Hoop cracking
	$2mm^{+++}$	7,2kV	0.014 0.005	0.03 0.08	0.47 0.06	Axial and hoop cracking
5mm x 3mm	$2mm^{++}$	7kV	Not measured			Hoop cracking
7mm x 7mm	2mm	5kV	-0.03	0.08	-0.375	No cracking initiation
	$2mm^{+}$	6kV	-0.12	0.22	-0.545	Hoop cracking

* the first number is the hollowing dimension in the axial direction of the cladding tube and the second gives the hollowing dimension in the circumferential direction.

** the initial curvature radius at the intersection between the hollowing and the die is 2mm then it was gradually increased through manual machining. The + signs indicates how many times the radius has been reworked.

a) 5x4 die, r=2mm, $\varepsilon_{zz} = 0.045$, $\varepsilon_{\theta\theta} = 0.18$

b) 4x5 die, r=2mm, $\varepsilon_{zz} = 0.1$, $\varepsilon_{\theta\theta} = 0.13$

c) 5x4 die, r=$2mm^{+++}$, $\varepsilon_{zz} = 0.08$, $\varepsilon_{\theta\theta} = 0.17$

d) 5x4 die, r=$2mm^{+++}$, $\varepsilon_{zz} = 0.06$, $\varepsilon_{\theta\theta} = 0.155$

Figure 2. Macrographic observation of the specimens after testing.

SIMULATION

In order to interpret the test a 3D finite element simulation was engaged.

Loading estimation

A simplified estimation of the loading is proposed below [8].

The magnetic field created by the capacitor discharge through the coil can be expressed by :

$$H = H_0 \exp\left(-\frac{t}{\tau}\right)\sin \omega t \qquad (1)$$

with t time, $\tau = 2L/R$ damping constant, $w = (LC)^{-1/2}$ pulsation and $H_0 = \frac{N}{l} V \sqrt{C/L}$ with N numbers of coil's spirals, l length of the coil, C generator capacity, L coil inductance (see Eq (2)), V generator supplying voltage, R resistance of the discharge circuit.

The coil inductance in case of a contiguous solenoid can be approached by :

$$L = \frac{\mu N \pi r^2}{\phi} * \left(0.1628 * \left(\frac{r}{N\phi}\right)^2 - 0.6238 * \left(\frac{r}{N\phi}\right) + 0.9786\right) \qquad (2)$$

with $\mu = \mu_0 . \mu_r$ the absolute permeability : μ_r the relative permeability is taken equal to 1 for the considered materials and $\mu_0 = 4\pi \times 10^{-7}\, H/m$ is the vacuum permeability, r radius of the coil's spirals, ϕ wire diameter, N numbers of coil's spirals.

As the magnetic field penetration depends on the pulsation and on the material conductivity , the electromagnetic pressure grows in a metal thickness named skin thickness. The skin thickness δ can be approximated through :

$$\delta = \frac{1}{\sqrt{\mu \pi f \gamma}} \qquad (3)$$

with γ the material conductivity.

The magnetic pressure grown in the skin thickness is :

$$P = \frac{\mu}{2} H_0^2 \exp\left(-\frac{2t}{\tau}\right)\sin^2 \omega t = \frac{\mu}{2}\left(\frac{N}{l} V \sqrt{C/L}\right)^2 \exp\left(-\frac{2t}{\tau}\right)\sin^2 \omega t \qquad (4)$$

As copper is highly conductive, the skin thickness δ is very small in the copper driver. Then, for simplicity's sake, we can considered the pressure given by Eq (5) as applied on the inner face of the driver. For the first simulations, the values taken for the different parameters are given in Table 2.

Table 2. Values of the different parameters used in order to evaluate the applied loading.

N	ϕ	l	r	C	V	R
10	1 mm	$N\phi$	4 mm	180 µF	5 kV	$4{,}2 \times 10^{-3}$ Ω

With this parameters set, the maximum pressure is equal to 5200 MPa and is reached in 14 µs.

Constitutive equations

For a start, simple constitutive equations were chosen in order to represent the behaviour of the copper driver and of a Zircaloy-4 alloy at the reception state at 20°C tested at high strain rates. The hardening is isotropic and is given point by point in Table 3 for copper and in Table 4 for Zircaloy-4. A von Mises criteria is used for the copper driver whereas a hill criteria was chosen for Zircaloy-4 in order to take into account material anisotropy (F=0.8118, G=1.089, H=1.0098). The elasticity is isotropic, the elastic modulus is equal to 95900 MPa (respectively 115000 MPa) and the Poisson coefficient is 0.37 (respectively 0.3) for Zircaloy-4 (respectively for copper). The die is rigid with an elastic modulus equal to 1.e9 MPa and a Poisson coefficient equal to 0.4.

Table 3. Isotropic plastic hardening for copper.

p	0	0.01	0.02	0.03	0.04	0.05	0.06	0.07	0.08	0.09	0.1	0.12	0.14	0.16	0.18	0.2	0.6	1
$R(p)$	136	127	152	169	183	194	203	211	219	226	232	243	254	263	271	278	371	425

Table 4. Isotropic plastic hardening for Zircaloy-4.

p	0	0.001	0.002	0.003	0.004	0.005	0.01	0.03	0.05	0.07	0.09	0.1	0.11	0.2	0.3	0.4
$R(p)$	682	943	933	981	991	999	1024	1065	1085	1092	1108	1112	1116	1140	1156	1168

In the future, the simulations will be conducted with a Lemaitre law identified for Zircaloy-4 in the temperature and strain rate ranges encountered during an RIA event.

Numerical modeling

The simulations are performed with a 3D formulation. At first, a parametric study was conducted with the finite element code Code_aster® in the framework of finite strains with an updated-Lagrangian formulation without friction between the contact zones. The influence of several parameters has been studied : mesh design, driver, hollowing design, curvature radius at the intersection between the hollowing and the die. The following conclusions from these first parametric simulations can be drawn.

- A mesh size equal to 120x120x190μm^3 ($\theta \times z \times r$) is at least necessary in order to have a fine determination of the strain biaxiality evolution.
- The curvature radius at the intersection between the hollowing and the die has a non negligible influence on the strain biaxiality at the centre of the hollowing. First the higher the curvature radius is, the less is the strain biaxiality ratio. At the end of the pressure ramp, the trend is reversed. In order to accurately interpret testing, a good knowledge of the curvature radius is required. A 3D profile measurement of the dies has been engaged.
- For the same level of pressure , the biaxiality ratio is decreased with the 5x4 die in comparison with the 4x5 die.
- Without taking into account friction between the contact zones, the simulation without the copper driver (the pressure ramp is then applied on the inner face of the specimen) leads to similar results to the one with the copper driver but the evolution of the different parameters is shifted forward as a function of the applied pressure.

Subsequently, in order to take into account contact with friction in 3D, the finite element code Zebulon® was used. A friction coefficient equal to 0.4 has been introduced. 4 simulations were conducted in the framework of finite strains with a corotational finite strain formulation based on an integrated rotation tensor : 5x4 die with and without friction and 4x5 die with and without copper driver and friction. As the 3D profile measurement of the die is not yet performed, the simulation were conducted with a curvature radius at the intersection between the hollowing and the die equal to 2mm.

Figure 3 shows the evolution during loading of strain biaxiality at the centre of the hollowing as a function of stress biaxiality (a) and as a function of time (b). The representative point of conventional ring tests, Penn State University (PSU) ring tests [9] and of the integral CABRI REP-Na tests are also reported on Figure 3a. The 4x5 die gives higher strain biaxiality ratios than the 5x4 die as it has been seen experimentally. The loading path obtained with this die is quite similar to the one calculated for the CABRI REP-Na tests with the SCANAIR code (which doesn't take into account the material anisotropy). It can be seen on Figure 3b that friction has a small influence on the loading path and tends to decrease the strain biaxiality ratio for the same pressure level. As it was seen during the parametric study, the loading path is also not very affected by the copper driver.

Figure 4 shows the evolution of the hoop strain as a function of the axial strain. The experimental fracture results are reported on this graphic and are in rather good agreement compared to the simulation considering the uncertainties found in the simulation (friction coefficient, 2mm curvature radius at the intersection between the hollowing and the die, constitutive equations not adapted to RIA conditions).

In order to study damage evolution during the test, the Rice and Tracey model [10] was applied as a post-treatment of the simulation. According to this model, the critical cavity growth rate is given by :

$$\left(\frac{R}{R_0}\right) = \exp \int 0.283 \exp\left(\frac{3}{2}\xi\right) \dot{\bar{E}} \qquad (5)$$

with R_0 the initial cavity radius, ξ the stress triaxiality and $\bar{E}$ the von Mises equivalent strain.

Figure 5 shows graphic visualisations of the initial mesh design (a), the von Mises equivalent stress (b), the cumulated plastic strain (c), the stress triaxiality (d), and the Rice and Tracey criteria (e) at 2.18µs for the 4x5 die with the copper driver and friction. The von Mises equivalent stress and the cumulated plastic strain are represented on the deformed mesh whereas the other quantities are represented on the non deformed mesh. The cumulated plastic strain is mainly localised on the outer face at the centre of the strain dome and on the inner face around the strain dome. The highest stress triaxiality is reached on the outer face at the center of the dome (≈ 0.6) and is twice lower on the inner face around the strain dome. Figure 5e shows that damage is mainly localised on the outer face at the center of the dome and on the inner face around the strain dome which is in agreement with the experimental cracking observed.

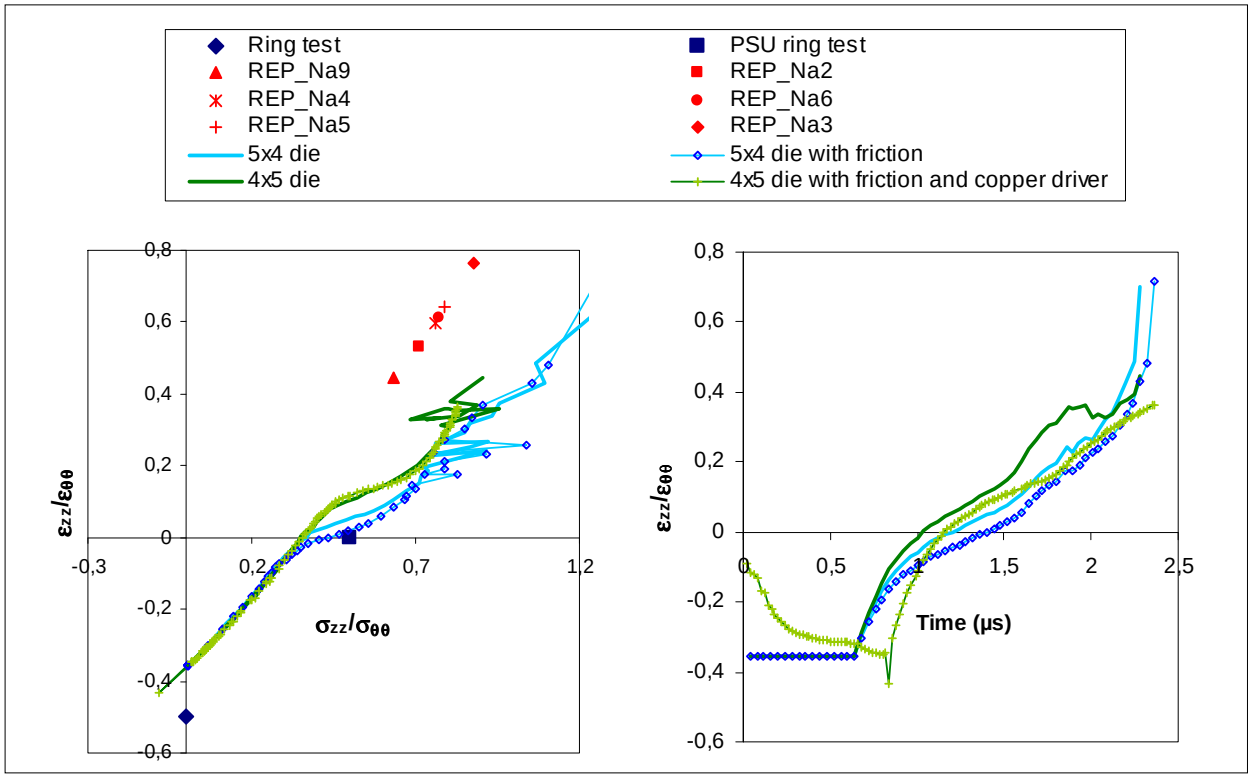

(a) as a function of stress biaxiality (b) as a function of time

Figure 3. Evolution of strain biaxiality at the centre of the hollowing during loading.

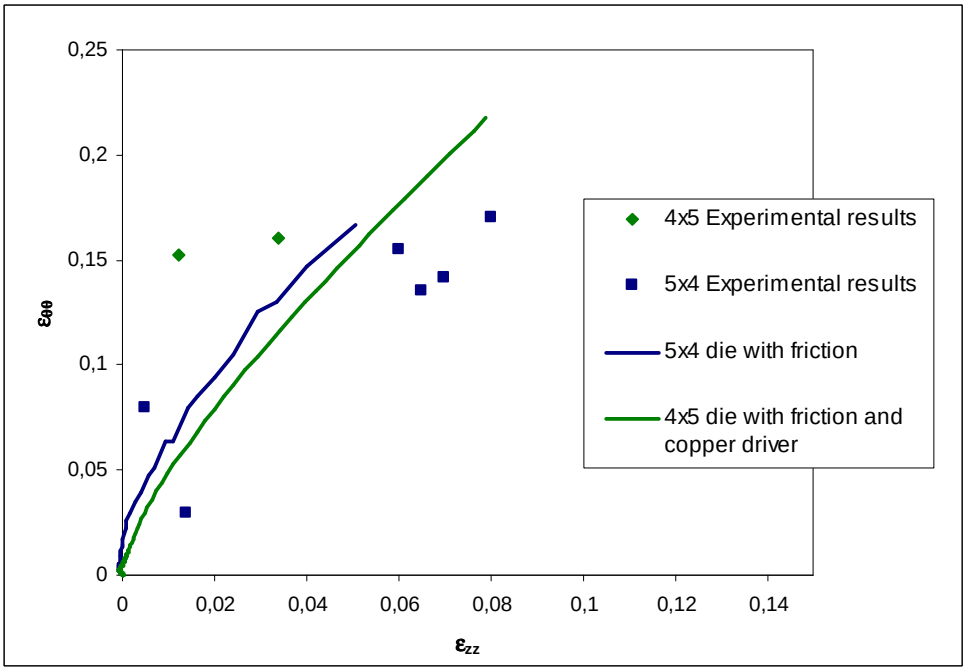

Figure 4. Evolution of the hoop strain as a function of the axial strain.

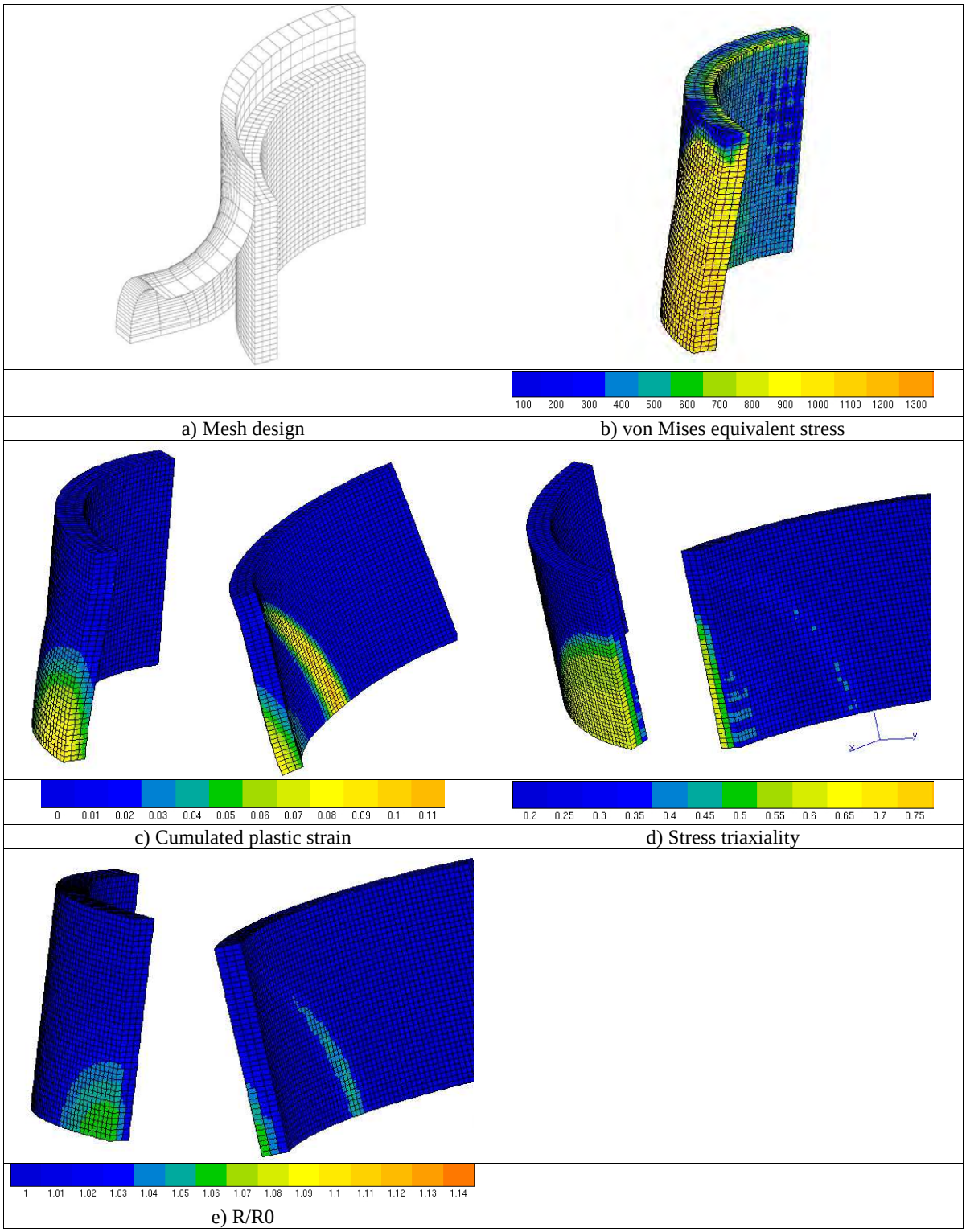

a) Mesh design

b) von Mises equivalent stress

c) Cumulated plastic strain

d) Stress triaxiality

e) R/R0

Figure 5. von Mises equivalent stress, the stress triaxiality and of the Rice and Tracey criteria for the 4x5 die at 2.18µs.

In the future, the simulation will be conducted with constitutive equations identified in the strain rate and temperature range adapted to RIA and testing conditions. The consistency of the analytical mechanical criteria developed from the PROMETRA database with the electromagnetic forming experimental results will be verified.

CONCLUSION

An experimental set up has been developed in order to characterize the fracture behavior of cladding tubes under RIA conditions. During an RIA, the cladding is in equibiaxial tension ($\varepsilon_{zz}/\varepsilon_{\theta\theta} = 1$) due to the loading imposed by the thermal expansion of the pellet. The typical strain rate expected for the cladding is $5s^{-1}$. The developed experimental set up is based on electromagnetic forming.

The development of the test and in particular of the die is delicate but leads to repeatable results with a controlled strain biaxiality ratio higher than those obtained through conventional tests such as ring tests or PSU ring tests. The use of electromagnetic forming process allows to test the specimen with very high strain rates. For the next test series other zircaloy alloys at the reception state and in hydrided conditions will be tested in order to look at hydrides influence on fracture strains.

A first finite element simulation of the test was engaged. The simulation and the experimental results are in quite good agreement. In the future, the consistency of the previously developed analytical mechanical criteria with the electromagnetic forming experimental results will be verified.

REFERENCES

1. E. Fédérici, F. Lamare, V. Bessiron, J. Papin : Status of development of the SCANAIR code for description of fuel behaviour under reactivity initiated accident, ANS international topical meeting on LWR fuel performance, Park City, April 9-12, 2000.
2. N. Waeckel, C. Bernaudat, B. Salles : EDF-proposed saferty domain for rod ejection accident in PWR, ANS international topical meeting on LWR fuel performance, Park City, April 9-12, 2000.
3. F. Schmitz, J. Papin : High burnup effects on fuel behaviour under accident conditions : the tests CABRI REP-Na, Journal of Nuclear Materials 270 (1999) 55-64
4. . Montgomery, N. Waeckel, R. Yang : Topical report on reactivity initiated accident : bases for RIA fuel and core coolability criteria, EPRI topical report # 1002865, 2002.
5. M. Balourdet, C. Bernaudat, V. Basini, N. Hourdequin : The PROMETRA programme – Assessment of mechanical properties of zircaloy-4 cladding during an RIA, SmiRT 15, Seoul, August 1999.
6. S. Leclercq, G. Rousselier and A. Parrot : Rupture of the fuel rod cladding under RIA conditions : A scheme to make the experimental mechanical data base representative of standard in-pile thermomechanical conditions, Proc., ANS international meeting on LWR fuel performance, Kyoto (2005).
7. P. Pupier and C. Bernaudat : A new analytical approach to study the rod ejection accident in PWRs, Proc., ANS international meeting on LWR fuel performance, Kyoto (2005).
8. M. Leroy, J.Y. Renaud : Travail des métaux en feuille, formage électromagnétique, Techniques de l'Ingénieur, traité Génie mécanique, B 7 582 –1.
9. T.M. link, D.A. Koss, A.T. Motta : Failure of Zircaloy cladding under Transverse plane-strain deformation, Nuclear Engineering and Desgin, vol. 186, pp. 379-394, 1998.
10. J.R. Rice and D.M. Tracey, J. Mech. Phys. Solids 17 (1969), p. 201.